Feasibility of ^{18}F-Sodium Fluoride PET/CT for Imaging of Atherosclerotic Plaque

Thorsten Derlin[1], Ulrich Richter[2], Peter Bannas[3], Philipp Begemann[3], Ralph Buchert[4], Janos Mester[1], and Susanne Klutmann[1]

[1]Department of Nuclear Medicine, University Medical Center Hamburg-Eppendorf, Hamburg, Germany; [2]Department of Anatomy II: Experimental Morphology, University Medical Center Hamburg-Eppendorf, Hamburg, Germany; [3]Department of Diagnostic and Interventional Radiology, University Medical Center Hamburg-Eppendorf, Hamburg, Germany; and [4]Department of Nuclear Medicine, Charite, Berlin, Germany

The aim of this study was to examine the prevalence, distribution, and topographic relationship of vascular ^{18}F-sodium fluoride uptake and arterial calcification in major arteries. **Methods:** Image data obtained from 75 patients undergoing whole-body ^{18}F-sodium fluoride PET/CT were evaluated retrospectively. Arterial radiotracer uptake and calcification were analyzed qualitatively and semiquantitatively. **Results:** ^{18}F-sodium fluoride uptake was observed at 254 sites in 57 (76%) of the 75 study patients, and calcification was observed at 1,930 sites in 63 (84%) of the patients. Colocalization of radiotracer accumulation and calcification could be observed in 223 areas of uptake (88%). However, only 12% of all arterial calcification sites showed increased radiotracer uptake. **Conclusion:** Our data indicate the feasibility of ^{18}F-sodium fluoride PET/CT for the imaging of mineral deposition in arterial wall alterations. ^{18}F-sodium fluoride PET/CT may provide relevant information about the morphologic and functional properties of calcified plaque.

Key Words: ^{18}F-sodium fluoride; plaque; atherosclerosis; calcification; PET; PET/CT

The formation and progression of atherosclerotic plaque are dynamic processes involving multiple pathophysiologic mechanisms, including inflammation, apoptosis, necrosis, and calcification. The composition and inflammatory state of plaque determine its stability and, therefore, the risk of clinical events (1–4).

Vascular calcification is a common phenomenon and possibly the most prominent feature of atherosclerosis (1,5). There is accumulating evidence that calcification in atherosclerotic plaque is an active, complex process exhibiting remarkable similarities to the formation of new bone (1,6). Cell types, signaling pathways, and metabolic compounds participating in bone formation have been found to be associated with plaque and arterial calcification (6–9). Pathologic mineralization can also occur through passive precipitation if physiologic inhibitors are no longer able to prevent mineral deposition (10).

Morphologic imaging techniques mainly provide information about structural aspects of calcified atherosclerotic lesions, such as the extent of plaque and the degree of stenosis, but fail to identify active calcification of plaque (11). For the reasons mentioned earlier, we postulated that ^{18}F-sodium fluoride PET/CT may have the potential to visualize ongoing mineral deposition in atherosclerotic plaque.

Therefore, the purpose of the present study was to assess the prevalence, location, and relationship of increased ^{18}F-sodium fluoride uptake and arterial calcifications and lesions.

MATERIALS AND METHODS

Study Population

From all subjects for whom whole-body ^{18}F-sodium fluoride PET/CT had been performed for the exclusion of bone metastases at the University Medical Center Hamburg-Eppendorf between December 2008 and July 2009, subjects were selected according to the following criteria. For inclusion, whole-body image data had to be digitally available for retrospective analysis. Subjects with systemic inflammatory disease, a history of vasculitis, a cardiovascular event in the preceding 3 mo, or chemotherapy in the preceding 2 mo were excluded. On the basis of these criteria, 75 subjects were included. Treatment with statins was recorded for all patients (12). A history of cardiovascular events (myocardial infarction or cerebrovascular insult) was obtained for every patient. All subjects had given written informed consent for the retrospective evaluation of their data.

Image Acquisition and Reconstruction

PET and CT were performed with a PET/CT hybrid system (Gemini GXL 10; Philips). ^{18}F-sodium fluoride was injected intravenously at a dose of 350 ± 50 MBq. During the 60-min uptake period, patients were hydrated orally with water. Imaging started with nonenhanced, low-dose CT of the whole body (120 kV, 80 mA). Next, PET of the whole body was performed for 90 s

TABLE 1. Prevalence, Distribution, and Intensity (SUV_{max}) of ^{18}F-Sodium Fluoride Uptake

Parameter	Value for:							
	Right common carotid artery	Left common carotid artery	Thoracic aorta	Abdominal aorta	Right iliac arteries	Left iliac arteries	Right femoral arteries	Left femoral arteries
No. of patients with ^{18}F-sodium fluoride uptake in artery wall	7 (9.3)	10 (13.3)	27 (36)	36 (48)	10 (13.3)	11 (14.7)	44 (58.7)	45 (60)
Total no. of uptake sites	8 (3.1)	10 (3.9)	47 (18.5)	70 (27.6)	11 (4.3)	14 (5.5)	46 (18.1)	48 (18.9)
SUV_{max}								
Mean ± SD	1.8 ± 0.5	2.0 ± 0.4	1.7 ± 0.5	2.0 ± 0.5	1.8 ± 0.7	2.1 ± 0.5	1.9 ± 0.6	1.7 ± 0.5
Range	1.3–2.6	1.5–2.7	0.8–3.0	1.2–3.5	1.0–3.3	1.5–3.4	1.1–3.6	1.0–3.2

Values in parentheses are percentages.

per bed position at the head and thorax and 60 s at the legs. Overlap between consecutive bed positions was 50%. Transverse PET slices were reconstructed into a 144 × 144 matrix with the iterative 3D line-of-response reconstruction algorithm of the system software. The low-dose CT was used for PET attenuation correction. The voxel size was 4 × 4 × 4 mm. The spatial resolution in the reconstructed PET images was about 8 mm in full width at half maximum.

Image Analysis

PET, CT, and PET/CT fusion images were evaluated both visually and semiquantitatively with the Extended Brilliance Workstation of the PET/CT system. The analysis was performed on the basis of lesions and on the basis of arterial segments. For the segment-based analysis, the major arteries were subdivided as follows: right and left common carotid arteries, ascending aorta, aortic arch, descending thoracic aorta, abdominal aorta, right and left iliac arteries, and right and left femoral arteries.

CT images were evaluated visually for the presence of abnormal sites of vascular calcification, defined as high-density mural areas. Each lesion was classified with scores on a scale for grading circumferential extent: 0, absent; 1, less than 25% of arterial wall circumference; 2, 25%−50% of arterial wall circumference; 3, 50%−75% of arterial wall circumference; and 4, greater than 75% of arterial wall circumference.

An arterial segment was categorized as having CT-positive results (CT+) if at least one calcified lesion was detected in it; otherwise, it was categorized as having CT-negative results (CT−). A CT+ segment was further classified with the maximum lesion score among all lesions in that segment.

Both attenuation-corrected and non–attenuation-corrected PET images were visually evaluated for focal lesions of increased radiotracer uptake. The locations of these areas in relation to the vascular wall and to calcification detected by CT were determined from PET/CT fusion images. A lesion was excluded from the analysis if it was suspected of being an artifact caused by spatial mismatching of PET and CT (physiologic organ or patient motion) or by activity spillover from extravascular structures. Semiquantitative analysis was performed by obtaining the maximum standardized uptake value (SUV_{max}). For focal lesions, an individual region of interest was placed around the atherosclerotic plaque. For linear lesions, SUV_{max}s were obtained from 4 representative, nonadjacent slices and then averaged. An arterial segment was categorized as having PET-positive results (PET+) if at least one PET lesion was detected in it.

Statistical Analysis

The prevalences of vascular calcification on CT images and increased vascular wall radiotracer uptake on PET images were calculated. The presence and locations of radiotracer uptake and

TABLE 2. Prevalence, Distribution, and Extent of Calcification in Studied Arterial Walls

Parameter	Value for:							
	Right common carotid artery	Left common carotid artery	Thoracic aorta	Abdominal aorta	Right iliac arteries	Left iliac arteries	Right femoral arteries	Left femoral arteries
No. of patients with calcification sites	17 (23)	23 (31)	47 (63)	57 (76)	45 (60)	50 (67)	50 (67)	51 (68)
No. of calcification sites	32 (2)	42 (2)	349 (18)	421 (22)	183 (9)	206 (11)	361 (19)	336 (17)
No. of calcification sites per affected segment (mean ± SD)	1.9 ± 1.1	1.8 ± 0.9	7.4 ± 6.5	7.4 ± 4.5	4.0 ± 2.9	4.1 ± 3.5	7.2 ± 6.0	6.6 ± 5.9
Calcification score for lesions coincident with ^{18}F-sodium fluoride uptake (mean ± SD)	1.8 ± 0.9	1.6 ± 0.7	1.7 ± 0.9	2.0 ± 1.1	3.0 ± 0.8	3.1 ± 1.0	1.7 ± 1.1	1.7 ± 1.2

Values in parentheses are percentages.

FIGURE 1. Transaxial ^{18}F-sodium fluoride PET/CT images of common iliac arteries in 67-y-old man. (A) CT image. (B) PET image. (C) Fused PET/CT image. ^{18}F-sodium fluoride accumulation in atherosclerotic lesion was colocalized with calcification. Arrows indicate calcified lesion.
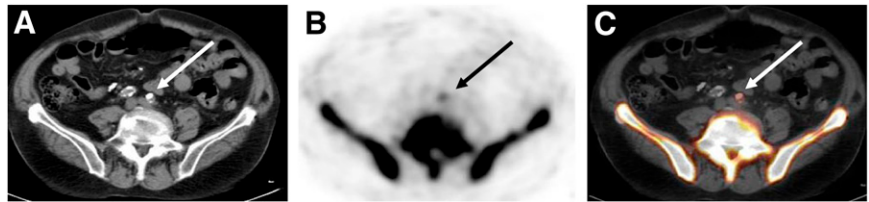
calcification on CT images were tested for association with the patients' clinical characteristics and abnormal vascular findings. Continuous variables were analyzed with the Student t test (2-sided) for unpaired data. For categoric data, P values were computed from contingency tables with the Fisher exact test. Statistical significance was established for P values of less than 0.05.

RESULTS

Patient Characteristics

The 75 recruited patients were 65.2 ± 12.3 (mean $\pm$ SD) y old and included 48 women. Nine patients had a history of previous cardiovascular events. Eight patients were receiving statins. The patients were clinically stable and asymptomatic when imaged.

Arterial Wall ^{18}F-Sodium Fluoride Uptake and Calcification

Arterial wall ^{18}F-sodium fluoride uptake was observed at 254 sites in 57 (76%) of the 75 study patients (Table 1). The prevalence was highest in the femoral arteries, followed by the abdominal aorta and thoracic aorta. SUV$_{max}$s ranged from 0.8 to 3.6. All sites of ^{18}F-sodium fluoride uptake were seen on both uncorrected and CT-based attenuation-corrected PET images.

Calcification was seen at 1,930 sites in 63 (84%) of the 75 study patients (Table 2). The prevalence of calcification was highest in the abdominal aorta, followed by the femoral and iliac arteries. The prevalence of ^{18}F-sodium fluoride accumulation was statistically significantly higher in lesions with extensive calcification than in those with only minor mineral deposition (the P value for CT calcification scores of 1 vs. 4 was <0.0001). No statistically significant association between intensity of radiotracer accumulation (SUV$_{max}$) and calcification score was found ($P = 0.71$). For 10 patients (13%), no arterial wall lesions were visualized by either PET or CT. Compared with the PET+ study population, these patients were significantly younger (53.4 ± 12.3 y vs. 69.1 ± 9.8 y; $P < 0.0001$).

No statistically significant correlation was found between prior administration of statins and the presence of vascular ^{18}F-sodium fluoride uptake ($P = 0.39$) or calcification ($P = 0.34$). The frequency of arterial calcification was higher in men (93%) than in women (79%) without reaching statistical significance ($P = 0.19$). The group of patients with vascular radiotracer uptake included more men (85%) than women (71%) without reaching statistical significance ($P = 0.26$). The presence of both vascular tracer accumulation and calcification was significantly associated with age ($P < 0.0001$). In all patients with a history of cardiovascular events, at least one site of increased ^{18}F-sodium fluoride uptake was observed (100% vs. 76% of the entire study population; $P = 0.10$).

Relationship Between ^{18}F-Sodium Fluoride Uptake and Calcification

Of the 600 total segments, 180 (30%) were PET+ and CT+, 160 (~27%) were PET negative (PET−) and CT+, 10 (~2%) were PET+ and CT−, and 250 (~42%) were PET− and CT−. The presence of arterial radiotracer accumulation was strongly associated with calcification within the vessel wall in these segments ($P < 0.0001$).

When the spatial correlation between vascular ^{18}F-sodium fluoride uptake and calcification sites in the studied arterial segments was analyzed on a per-lesion basis, only 31 (12%) of the 254 lesions with marked arterial wall ^{18}F-sodium fluoride uptake did not show concordant calcification. For the remaining 223 lesions with uptake (88%), a correspondence of radiotracer accumulation and calcification was observed. However, only these 223 (12%) of the 1,930 total calcification sites showed prominent ^{18}F-sodium fluoride uptake in at least some part of the calcified plaque. Examples of arterial wall calcification coincident with ^{18}F-sodium fluoride uptake are shown in Figures 1 and 2.

DISCUSSION

Our results indicate the feasibility of using ^{18}F-sodium fluoride for the in vivo functional imaging of atherosclerotic

FIGURE 2. Transaxial ^{18}F-sodium fluoride PET/CT images of aortic arch in 76-y-old woman. (A) CT image. (B) PET image. (C) Fused PET/CT image. ^{18}F-sodium fluoride uptake in atherosclerotic lesion coincided with calcification. Arrows indicate calcified lesion.
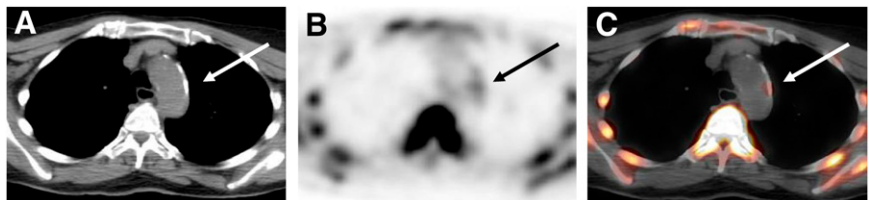
lesions. The arterial wall ^{18}F-sodium fluoride distribution was consistent with established atherosclerotic topography, with increased uptake in the thoracic aorta and at the carotid bifurcation.

Both active and passive mechanisms of calcium deposition may explain arterial calcification. Plaque mineralization may be caused by passive calcium precipitation associated with areas of advanced tissue degeneration or necrosis, which can frequently be observed in advanced atherosclerotic lesions (1,10). There is growing evidence that plaque calcification is an active process akin to bone formation. Atheromatous lesions and fibrocalcific plaques express proteins and possess cell types (i.e., chondrocytes, osteoblasts, and osteoclasts) and signaling pathways normally associated with bone and may contain bonelike tissues (6–9). Although the precise mechanism of ^{18}F-sodium fluoride uptake is not fully known yet, one may assume that it indicates ongoing active mineral deposition in atherosclerotic lesions. Plaques still accumulating ^{18}F-sodium fluoride might not represent stable, nonprogressive stages of disease.

With regard to the colocalization of tracer accumulation and calcification sites, the results of the present study differ substantially from the findings of studies of other tracers, such as ^{18}F-FDG (13–15). Although existing studies are difficult to compare because of differences in inclusion criteria, in the portion of the arterial vasculature evaluated, and in data analysis, most of them reported no colocalization of radiotracer uptake and calcification. Using ^{18}F-FDG, Dunphy et al. (14) and Ben-Haim et al. (15) found colocalization in less than 2% of cases and in 7% of sites, respectively. Bucerius et al. (16) observed no ^{18}F-fluoromethylcholine uptake in completely calcified lesions, and Kato et al. (17) found ^{11}C-choline uptake in less than 1% of calcification sites. In the present study, the correlation of radiotracer uptake and arterial wall calcification indicated that 88% of the lesions with ^{18}F-sodium fluoride uptake showed concordant calcification. Unlike ^{18}F-FDG or choline derivatives, ^{18}F-sodium fluoride may provide new insights into the functional properties of calcified lesions.

The present study had some limitations. First, the lack of synchronization of PET image acquisition with both the cardiac cycle and the spontaneous respiration rate might have affected the visualization of arterial uptake, particularly with regard to the coronary arteries, the ascending aorta, and the aortic arch (18). Second, dynamic and delayed data could provide relevant additional information regarding the nature of arterial radiotracer uptake (19,20). Third, the limited spatial resolution of PET renders images subject to partial-volume effects, which might lead to an underestimation of tracer accumulation in atherosclerotic plaque, especially in smaller arteries. Finally, because of the retrospective nature of the present study, histologic evaluation of the detected plaque could not be performed. Therefore, data concerning the structure, exact composition, and stability of the atherosclerotic lesions are not available. Further prospective studies are needed to determine the prognostic value of tracer uptake and to determine whether it might effectively target therapeutic interventions to influence clinical outcomes.

CONCLUSION

We demonstrated the feasibility of using ^{18}F-sodium fluoride for the imaging of arterial wall alterations. ^{18}F-sodium fluoride PET/CT may provide relevant additional information regarding plaque physiology.

REFERENCES

1. Doherty TM, Asotra K, Fitzpatrick LA, et al. Calcification in atherosclerosis: bone biology and chronic inflammation at the arterial crossroads. *Proc Natl Acad Sci USA.* 2003;100:11201–11206.
2. Chen W, Bural GG, Torigian DA, Rader DJ, Alavi A. Emerging role of FDG-PET/CT in assessing atherosclerosis in large arteries. *Eur J Nucl Med Mol Imaging.* 2009;36:144–151.
3. van der Wal AC, Becker AE, van der Loos CM, Das PK. Site of intimal rupture or erosion of thrombosed coronary atherosclerotic plaques is characterized by an inflammatory process irrespective of the dominant plaque morphology. *Circulation.* 1994;89:36–44.
4. Fuster V, Lewis A. Conner Memorial Lecture: mechanisms leading to myocardial infarction—insights from studies of vascular biology. *Circulation.* 1994;90:2126–2146.
5. Detrano RC, Doherty TM, Davies MJ, Stary HC. Predicting coronary events with coronary calcium: pathophysiologic and clinical problems. *Curr Probl Cardiol.* 2000;25:374–402.
6. Jeziorska M, McCollum C, Wooley DE. Observations on bone formation and remodelling in advanced atherosclerotic lesions of human carotid arteries. *Virchows Arch.* 1998;433:559–565.
7. Engelse MA, Neele JM, Bronckers AL, Pannekoek H, de Vries CJ. Vascular calcification: expression patterns of the osteoblast-specific gene core binding factor alpha-1 and the protective factor matrix Gla protein in human atherogenesis. *Cardiovasc Res.* 2001;52:281–289.
8. Luo G, Ducy P, McKee MD, et al. Spontaneous calcification of arteries and cartilage in mice lacking matrix GLA protein. *Nature.* 1997;386:78–81.
9. Dhore CR, Cleutjens JP, Lutgens E, et al. Differential expression of bone matrix regulatory proteins in human atherosclerotic plaques. *Arterioscler Thromb Vasc Biol.* 2001;21:1998–2003.
10. Schinke T, McKee MD, Karsenty G. Extracellular matrix calcification: where is the action? *Nat Genet.* 1999;21:150–151.
11. Fayad ZA, Fuster V, Nikolaou K, Becker C. Computed tomography and magnetic resonance imaging for noninvasive coronary angiography and plaque imaging: current and potential future concepts. *Circulation.* 2002;106:2026–2034.
12. Tahara N, Kai H, Ishibashi M, et al. Simvastatin attenuates plaque inflammation: evaluation by fluorodeoxyglucose positron emission tomography. *J Am Coll Cardiol.* 2006;48:1825–1831.
13. Ogawa M, Ishino S, Mukai T, et al. ^{18}F-FDG accumulation in atherosclerotic plaques: immunohistochemical and PET imaging study. *J Nucl Med.* 2004;45: 1245–1250.
14. Dunphy MP, Freiman A, Larson SM, Strauss HW. Association of vascular ^{18}F-FDG uptake with vascular calcification. *J Nucl Med.* 2005;46:1278–1284.
15. Ben-Haim S, Kupzov E, Tamir A, Israel O. Evaluation of ^{18}F-FDG uptake and arterial wall calcifications using ^{18}F-FDG PET/CT. *J Nucl Med.* 2004;45:1816–1821.
16. Bucerius J, Schmaljohann J, Bohm I, et al. Feasibility of ^{18}F-fluoromethylcholine PET/CT for imaging of vessel wall alterations in humans: first results. *Eur J Nucl Med Mol Imaging.* 2008;35:815–820.
17. Kato K, Schober O, Ikeda M, et al. Evaluation and comparison of ^{11}C-choline uptake and calcification in aortic and common carotid arterial walls with combined PET/CT. *Eur J Nucl Med Mol Imaging.* 2009;36:1622–1628.
18. Alsaid H, Sabbah M, Bendahmane Z, et al. High-resolution contrast-enhanced MRI of atherosclerosis with digital cardiac and respiratory gating in mice. *Magn Reson Med.* 2007;58:1157–1163.
19. Menezes LJ, Kotze CW, Hutton BF, et al. Vascular inflammation imaging with ^{18}F-FDG PET/CT: when to image? *J Nucl Med.* 2009;50:854–857.
20. Davies JR, Rudd JH, Fryer TD, et al. Identification of culprit lesions after transient ischemic attack by combined ^{18}F fluorodeoxyglucose positron-emission tomography and high-resolution magnetic resonance imaging. *Stroke.* 2005;36: 2642–2647.